Direct Dimethyl Ether Synthesis by Spatial Patterned Catalyst Arrangement: A Modeling and Simulation Study

Kevin McBride, Thomas Turek and Robert Güttel
Institute of Chemical Process Engineering, Clausthal University of Technology, 38678 Clausthal-Zellerfeld, Germany

DOI 10.1002/aic.13730
Published online January 13, 2012 in Wiley Online Library (wileyonlinelibrary.com).

The effect of spatially patterned catalyst beds was investigated using direct dimethyl ether (DME) synthesis from synthesis gas as an example. A layered arrangement of methanol synthesis (MS) and dehydration catalyst was chosen and studied by numerical simulation under typical operating conditions for single-step DME synthesis. It was revealed that catalyst layers significantly influence the DME productivity. With an increasing number of layers from two to 40, an increase in DME productivity was observed approaching the performance of a physical catalyst mixture for an infinite number of layers. The results prove that a physical mixture of MS and dehydration catalyst achieves the highest DME productivity under operating conditions chosen in this study. Essentially, the layered catalyst arrangement is comparable to a cascade model of the two-step process, which is less efficient in terms of DME yield than the single-step process. However, the layered catalyst arrangement could be beneficial for other reaction systems. © 2012 American Institute of Chemical Engineers *AIChE J,* 58: 3468–3473, 2012
Keywords: chemical reactors, mathematical modeling, micropacked-bed reactor, reaction engineering, simulation

Introduction

Several reactions, such as methanol synthesis (MS), are limited by equilibrium constraints. To overcome these restrictions, it could be beneficial to introduce an additional catalyst to facilitate an auxiliary reaction to shift the overall equilibrium toward valuable products. Both catalysts can be arranged in a physical mixture or spatially structured, such as in layers. Cote et al.[1,2] studied this strategy for spatially layered catalyst patterns from a general point of view and proposed that a reduction in performance limitations is possible with the introduction of an additional catalyst or by separating mixed catalyst beds.

In this article, we apply this strategy to the equilibrium-limited MS by addition of a second catalyst active for methanol dehydration (MD) to dimethyl ether (DME). The physical mixture of MS and dehydration catalyst is discussed in literature under the headline direct DME synthesis. It is reported that the yield of valuable products (methanol and DME) can be significantly increased by combining both reactions within a single reactor.[3] Alternatively, a layered catalyst arrangement could also improve the productivity of the combined MS and dehydration. For the example of combined Fischer-Tropsch synthesis (FTS) and product upgrade, Gormley et al.[4] showed that a layered catalyst arrangement is beneficial over a physical catalyst mixture in terms of low methane and heavy hydrocarbon selectivity. These interesting results are our motivation for studying the effect of spatial patterned catalyst arrangement in the combined MS and dehydration reaction.

Correspondence concerning this article should be addressed to R. Güttel at guettel@icvt.tu-clausthal.de.
This paper was presented at the DGMK-Conference "Catalysis—Innovative Applications in Petrochemistry and Refining" in October 2011 at Dresden, Germany.

This work is based on the modeling of the MS and dehydration reactions in a fixed-bed reactor. The effect of a spatially patterned catalyst arrangement was studied for different numbers of catalyst layers and compared to a physical catalyst mixture. Two cases were investigated. In one case, the reaction was allowed to approach equilibrium by the end of the reactor, while for the second case, equilibrium was not reached within any catalyst layer.

Background

Reaction network

The direct synthesis of DME from synthesis gas proceeds with methanol as an intermediate.[5] Usually, MS from synthesis gas occurs in the presence of copper-based catalysts, where CO or CO_2 is converted to methanol (Eqs. 1 and 2). Under MS conditions, the water gas shift (WGS) reaction also occurs (Eq. 3). The MD to DME is carried out on acidic catalysts, such as the widely studied γ-alumina (Eq. 4). This catalyst can be assumed to be inactive for the WGS reaction. Both catalysts were investigated in the same reactor that was either well mixed or spatially patterned.

$$CO_2 + 3H_2 \Leftrightarrow CH_3OH + H_2O \quad (1)$$

$$CO + 2H_2 \Leftrightarrow CH_3OH \quad (2)$$

$$CO_2 + H_2 \Leftrightarrow CO + H_2O \quad (3)$$

$$2CH_3OH \Leftrightarrow CH_3OCH_3 + H_2O \quad (4)$$

To help understand the complex nature of the reaction network, Scheme 1 is provided to show the network for each element involved. In principle, hydrogen, oxygen, and carbon can be fed to the system by H_2, H_2O, CO, and CO_2.

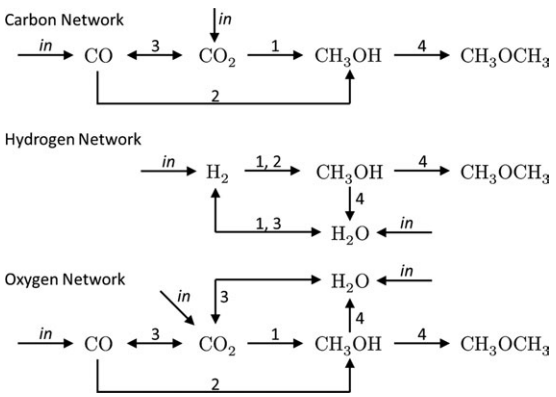

Scheme 1. Reaction network for involved elements (1: MS from CO_2; 2: MS from CO; 3: WGS reaction; 4: methanol dehydration to DME).

Methanol and DME are the valuable products of the process. The figure shows that carbon follows basically a linear path from CO/CO_2 to DME. It has to be mentioned that the formation of methanol proceeds predominantly via hydrogenation of CO_2,[6,7] which is formed from CO and H_2O by WGS. The hydrogen network is similar in that most of the H_2 fed to the system ends up in DME or methanol. The oxygen network is more complicated as the oxygen fed to the system is only partially incorporated into the final products, which is obvious comparing the C/O ratios of feed and product species. Oxygen not incorporated into the valuable products appears as water, which affects the formation rate of methanol and DME both by kinetic inhibition and by equilibrium limitation. In contrast, a certain CO_2 concentration at the reactor inlet enhances the MS reaction rate. In conclusion, oxygen inventory in the system appears to be the key influence on the equilibrium yield and methanol formation rate and should be optimized.

Patterned catalyst arrangement

To our knowledge, spatially patterned catalyst arrangements in packed-bed reactors (Figure 1) are rarely described in literature. Most papers deal with the performance of two consecutive reactions within one reactor, thus, using a system with only two catalyst layers. One example is the combination of FTS and product upgrade within one single reactor as investigated by Schaub and coworkers.[8,9] A systematic investigation of spatially patterned packed-bed reactors with more than two catalyst layers was published by Cote et al.[1,2,10] Cote investigated this topic for hypothetical reaction systems and the results show that spatially organized catalysts may improve the overall reactor performance. However, the interesting findings from Cote are not yet confirmed by real reaction networks, neither experimentally nor by modeling and simulation. For this reason, we pick up the idea of spatially patterned packed-bed reactors and transfer it to the interesting direct synthesis of DME from synthesis gas.

Reactor Modeling

Reaction kinetics

The reaction network can be described by the key reactions 1, 3, and 4.[5] The kinetic equations for MS from CO_2 and for WGS reaction were taken from Bussche and Froment.[6] The kinetics of MD to DME on γ-Al_2O_3 is described by the approach of Bercic et al.[11,12] The equilibrium constant for MD was taken from Diep and Wainwright.[13] The equilibrium of the reaction network was verified using a Gibb's reactor model from Aspen Plus®. Below, the kinetic equations are summarized. The kinetic parameters can be found in the Appendix.

(1) Methanol (MeOH) synthesis

$$r_{\mathrm{MeOH}} = k_1 \frac{p_{\mathrm{H_2}} p_{\mathrm{CO_2}} \left(1 - \frac{1}{K_{\mathrm{eq1}}} \frac{p_{\mathrm{MeOH}} p_{\mathrm{H_2O}}}{p_{\mathrm{CO_2}} p_{\mathrm{H_2}}^3}\right)}{\left(1 + K_2 \left(\frac{p_{\mathrm{H_2O}}}{p_{\mathrm{H_2}}}\right) + \sqrt{K_3 p_{\mathrm{H_2}}} + K_4 p_{\mathrm{H_2O}}\right)^3} \quad (5)$$

(2) WGS reaction

$$r_{\mathrm{WGS}} = k_5 \frac{p_{\mathrm{CO_2}} \left(1 - K_{\mathrm{eq2}} \frac{p_{\mathrm{CO}} p_{\mathrm{H_2O}}}{p_{\mathrm{CO_2}} p_{\mathrm{H_2}}}\right)}{\left(1 + K_2 \left(\frac{p_{\mathrm{H_2O}}}{p_{\mathrm{H_2}}}\right) + \sqrt{K_3 p_{\mathrm{H_2}}} + K_4 p_{\mathrm{H_2O}}\right)} \quad (6)$$

(3) Methanol dehydration

$$r_{\mathrm{DME}} = k_6 K_7^2 \frac{c_{\mathrm{MeOH}}^2 - \frac{c_{\mathrm{H_2O}} c_{\mathrm{DME}}}{K_{\mathrm{eq3}}}}{\left(1 + 2\sqrt{K_7 c_{\mathrm{MeOH}}} + K_8 c_{\mathrm{H_2O}}\right)^4} \quad (7)$$

Reactor model

The simulations were carried out based on a standard one-dimensional heterogeneous fixed-bed reactor model comprising heat and mass balances (Eqs. 8–10), which was implemented in Matlab using the ode15s solver.

(1) Mass balance in the gas phase

$$0 = -u_{\mathrm{G},0} \frac{\partial}{\partial z} c_{\mathrm{G},i} - k_{\mathrm{AGS},i} (c_{\mathrm{G},i} - c_{\mathrm{S},i}) \quad (8)$$

(2) Mass balance at the catalyst surface

$$0 = k_{\mathrm{AGS},i} (c_{\mathrm{G},i} - c_{\mathrm{S},i}) + x_{\mathrm{cat}} \sum_j \eta_{\mathrm{eff},j} \nu_{i,j} r_j \quad (9)$$

(3) Heat balance

$$0 = -c_{p,\mathrm{G}} \rho_{\mathrm{G}} u_{\mathrm{G},0} \frac{\partial}{\partial z} T - \frac{4}{d_{\mathrm{R}}} h_{\mathrm{ov}} (T - T_{\mathrm{w}}) + x_{\mathrm{cat}} \sum_j \eta_{\mathrm{eff},j} r_j \Delta_{\mathrm{R}} H_j \quad (10)$$

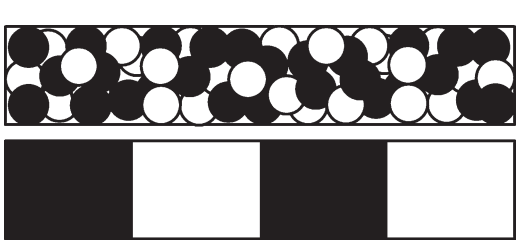

Figure 1. Spatially patterned catalyst bed; top: well mixed bed and bottom: layered arrangement; black: catalyst 1 and white: catalyst 2 (modified from Ref. 2).

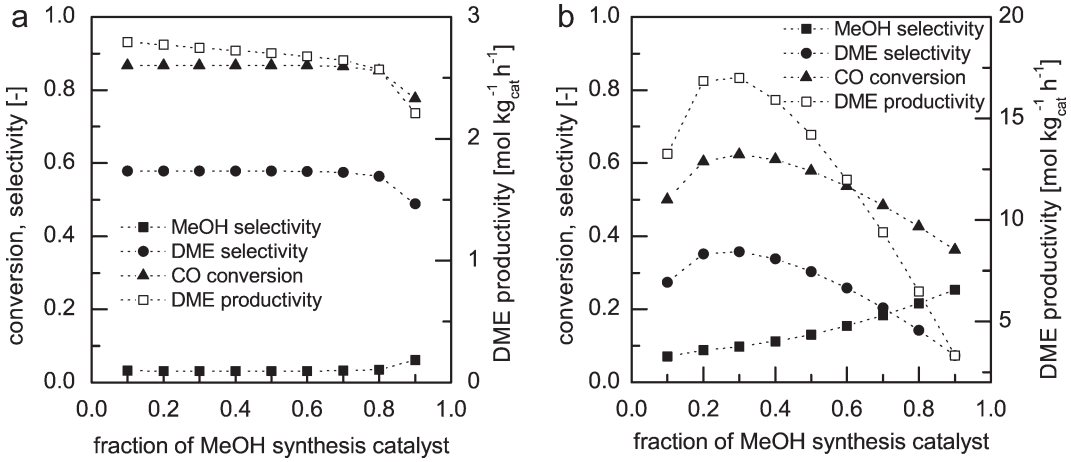

Figure 2. Effect of volume fraction of MeOH synthesis and dehydration catalyst on CO conversion, MeOH and DME selectivity, and DME productivity (left: equilibrium case and right: kinetic case).

The physical properties, heat-, and mass-transfer rates were calculated with correlations from VDI Wärmeatlas,[14] according to our previous work.[15,16] Diffusion coefficients were calculated according to Onken et al.[17] Axial dispersion was neglected due to the high Bodenstein numbers of more than 100. For simplicity reasons, a constant volumetric flow rate was assumed.

Layers

The core of this work is the effect of a patterned catalyst arrangement for direct DME synthesis. For this purpose, the catalyst layers were modeled using factors f_i that determine the volume fraction of each catalyst i in the reactor or in a specific layer. The factors are variable in axial direction between 0 and 1 and represent the volume fraction of both catalysts within one volume element. The reaction rates in each layer are controlled by multiplication with the corresponding factor f_i for the actual axial position. MS and dehydration catalysts are arranged separately from each other, beginning with synthesis catalyst at the reactor inlet and ending with dehydration catalyst at the outlet. The total number of layers is determined by counting each catalyst layer. For example, two layers means one layer of synthesis and dehydration catalyst, respectively.

Simulation conditions

Two types of simulation campaigns were conducted. First, the model was verified with literature data. The simulations show a good agreement with literature data from Bussche and Froment and Bercic et al.[6,11,12] in terms of temperature profile and conversion.

For studying the intrinsic effect of spatial patterned catalyst beds, isothermal conditions were assumed to avoid overlaying temperature effects. To eliminate internal mass-transfer limitations, a micropacked-bed reactor was chosen as it was recently proposed for direct DME synthesis.[18,19] For the present example, the reactor length was 1 m, the channel diameter was 3 mm, and the catalyst particle size was 300 μm. Because of different catalyst density, the catalyst inventory within one layer was 1775 and 1634 kg_{cat} m^{-3} for MS and dehydration catalyst, respectively. Simulations were carried out for equal height of each catalyst layer, meaning a volume fraction of 0.5 for synthesis and dehydration catalyst within the reactor, respectively.

Two basic cases were simulated to study the effect of layered catalyst bed. In case 1, equilibrium was reached at reactor outlet (equilibrium case), while case 2 remains in the kinetic range (kinetic case). This was achieved by increasing the space velocity from 650 to 6500 L_{STP} kg_{cat}^{-1} h^{-1}. The operation conditions at the inlet for the basic cases are 540

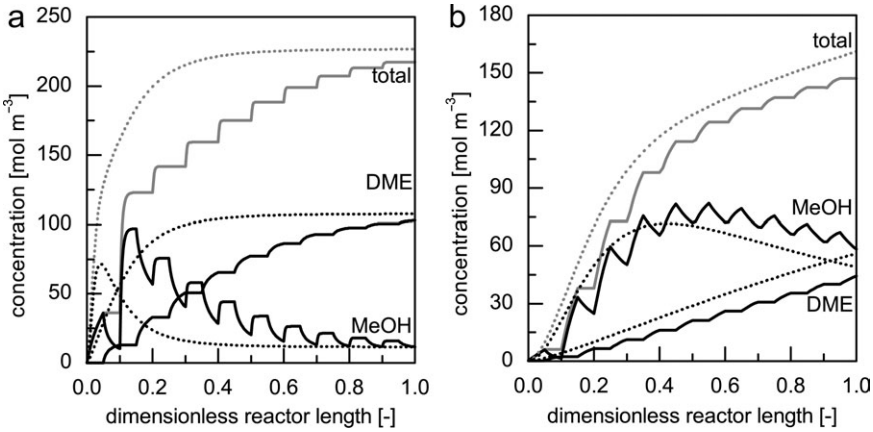

Figure 3. Concentration profiles of methanol, DME, and total converted CO (2× DME plus methanol) for 20 layers (solid lines) and a physical catalyst mixture (dotted lines) (left: equilibrium case and right: kinetic case).

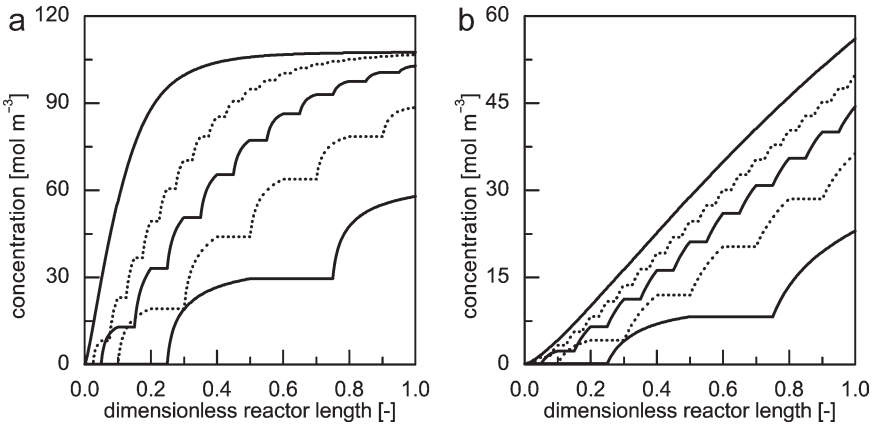

Figure 4. Concentration profiles of DME for 4, 10, 20, and 40 layers and a physical catalyst mixture (from bottom to top; left: equilibrium case and right: kinetic case).

K and 50 bar, and the molar H_2/CO ratio is 2. The mole fractions of CO_2 and H_2O at the inlet were set to 1×10^{-4} and for methanol and DME to 0. To quantify the conversion and selectivity, following equations were used (Eqs. 11–13)

$$X_{CO} = \frac{c_{CO}^{in} - c_{CO}^{out}}{c_{CO}^{in}} \tag{11}$$

$$S_{MeOH} = \frac{c_{MeOH}^{out}}{c_{MeOH}^{in} + c_{CO}^{in} + c_{CO_2}^{in} + 2c_{DME}^{in}} \tag{12}$$

$$S_{DME} = \frac{2c_{DME}^{out}}{c_{MeOH}^{in} + c_{CO}^{in} + c_{CO_2}^{in} + 2c_{DME}^{in}} \tag{13}$$

Results and Discussion

The reaction rates of MS and dehydration may differ. For this reason, it is of interest to see if an optimal catalyst mixture exists that would maximize reactor productivity. In Figure 2, the effect of the composition of a physical catalyst mixture on conversion, selectivity, and productivity is shown. At the ordinate, the volume fraction of the MeOH synthesis catalyst is given. The difference to unity is covered by the MeOH dehydration catalyst.

For the equilibrium case, conversion and selectivity are not affected until a synthesis catalyst fraction of 0.8. At this point, the amount of dehydration catalyst is not enough to reach equilibrium anymore and CO conversion decreases. As a result, the methanol production rate is higher than the dehydration rate and MeOH selectivity increases while DME selectivity decreases. The linear decline in DME productivity at synthesis catalyst fractions up to 0.8 can be explained by the change in overall catalyst density, due to higher synthesis catalyst density.

For the kinetic case, a pronounced optimum in DME productivity could be observed at a synthesis catalyst fraction of about 0.3. At lower synthesis catalyst fractions, methanol production rate is less than dehydration rate, while at higher catalyst fractions, the dehydration rate is too slow. The strong dependency of DME productivity on catalyst mixture in the kinetic range could be explained by the fact that kinetics rather than equilibrium control the chemical conversion. The DME productivity in the kinetic case is higher than in the equilibrium case due to the more efficient use of the catalyst.

The effect of the layered catalyst arrangement on the concentration profiles of methanol and DME is shown in Figure 3 and compared to a physically mixed catalyst bed. Additionally, the carbon concentration of DME and MeOH is shown (curve "total").

In the first layer, methanol is formed and methanol concentration increases. In the second layer, methanol is consumed to form DME, thus, methanol concentration decreases

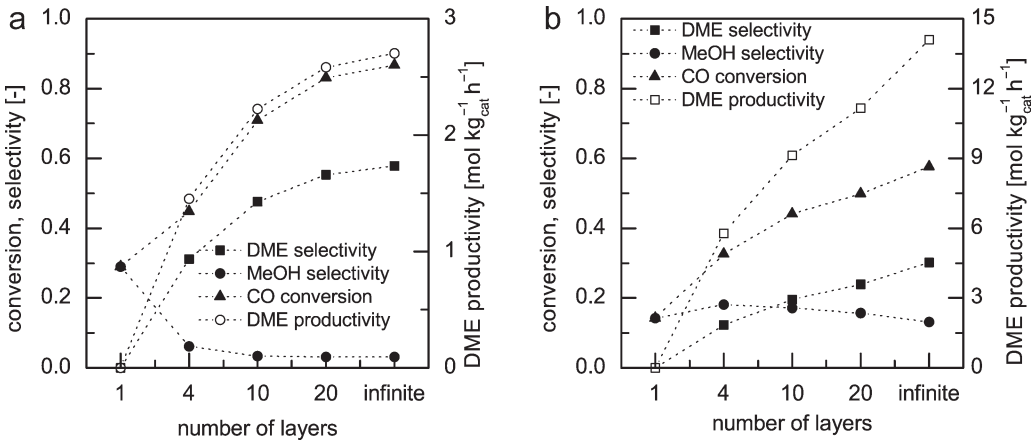

Figure 5. Effect of the number of catalyst layers on CO conversion, MeOH and DME selectivity, and DME productivity (left: equilibrium case and right: kinetic case).

Table 1. Kinetic Parameters

Parameter	Dimension	A_i	B_i	Reference
k_1	mol kg_{cat}^{-1} s^{-1} bar^{-2}	1.07	36,696	6
K_2	–	3453.38	–	6
K_3	bar^{-1}	0.499	17,197	6
K_4	bar^{-1}	6.62×10^{-11}	124,119	6
k_5	mol kg_{cat}^{-1} s^{-1} bar^{-1}	1.22×10^{10}	−94,765	6
k_6	kmol kg_{cat}^{-1} h^{-1}	5.35×10^{13}	−17,280	11,12
K_7	m^3 $kmol^{-1}$	5.39×10^{-4}	8487	11,12
K_8	m^3 $kmol^{-1}$	8.47×10^{-2}	5070	11,12

and DME concentration increases. In the third layer, methanol is formed again and DME concentration remains constant, as no dehydration activity is present in this layer. The remaining layers can be described accordingly. The summation of total carbon atom concentration from methanol and DME results in a stair-shaped curve. The increase in concentration is caused by methanol formation in the synthesis layer. In the dehydration layer, no further educt is converted, but methanol is transformed into DME. Thus, the concentration of carbon in the valuable products remains constant in this layer. A comparison with the physical catalyst mixture shows that the concentration of DME and the valuable product is lower in the layered catalyst bed and that the concentration of methanol is higher. This observation holds for both the equilibrium and the kinetic case.

The effect of number of layers is shown in Figure 4 for DME as an example. It can be seen that the DME concentration at the reactor outlet increases with increasing number of layers resulting in a higher DME productivity. This can be explained by the fact that a physical catalyst mixture is essentially identical with a layered catalyst bed consisting of infinite number of layers with differential height. The same trend holds for both the equilibrium and the kinetic case.

In Figure 5, the effect of the number of catalyst layers on conversion, selectivity, and productivity is shown. The left part of Figure 5 shows the results for the equilibrium case and on the right the kinetic case is displayed. It is obvious that increasing the number of layers influences conversion, selectivity, and productivity. While methanol selectivity decreases, the DME selectivity and CO conversion increase with increasing number of layers. Consequently, a higher DME productivity can be reached with a larger number of layers. This means that approaching a physical mixture of MS and dehydration catalyst yields in higher DME productivity. The case for one single catalyst layer represents MS only, without MD. Obviously, CO conversion is smaller due to equilibrium constraints. A direct comparison of both cases shows that in the kinetic range the DME productivity is higher than in the equilibrium case, even though the CO conversion and DME selectivity is less. This can be explained by the fact that in the kinetic range the catalyst usage is higher, as the system is not limited by near-equilibrium conditions. Optimizing the fraction of MS and dehydration catalyst by nonequal catalyst layer lengths could further improve the DME productivity according to our results shown in Figure 2. However, it is unlikely that the layered catalyst arrangement will exceed the physical mixture in terms of productivity for the same catalyst bed composition.

Conclusions

In this article, we present a simulation study on spatially patterned packed catalyst beds. As an example, the direct synthesis of DME from synthesis gas was chosen due to the main reaction path being characterized by a consecutive reaction via methanol as an intermediate. Both reactions are catalyzed by different catalysts, but operating conditions for both are comparable, making a layered catalyst arrangement feasible.

It was observed that a layered catalyst arrangement significantly influences CO conversion and methanol and DME yield compared to a physical catalyst mixture. Increasing the number of layers leads to an increase in conversion and yield. Finally, an infinite number of layers will approach the values for the physical catalyst mixture. Consequently, the layered catalyst arrangement with a finite number of layers could not achieve DME space time yield of a well-mixed bed. This observation can be explained by the higher average methanol concentration for the layered catalyst arrangement and, thus, stronger equilibrium constraints for the MS reaction. In conclusion, the layered catalyst arrangement represents a cascade of the two-step DME synthesis process, which is known to be less productive than the single-step process. However, it cannot be excluded that other processes may profit from a layered catalyst bed, as a significant effect was found in this study. Cote et al. propose that reaction networks with different operating temperature ranges or incompatibilities between chemical species and one catalyst may be interesting candidates for the discussed spatially patterned catalyst beds.[1]

Acknowledgment

Robert Güttel thanks "Fonds der Chemischen Industrie", Germany for financial support.

Notation

c_G = concentration, gas phase, mol m^{-3}
c_S = concentration, solid phase, mol m^{-3}
$c_{p,G}$ = heat capacity, J kg^{-1} K^{-1}
d_R = reactor diameter, m
f = factor for catalyst layers
h_{ov} = overall radial heat-transfer coefficient, W m^{-2} K^{-1}
k, K, A, B = kinetic parameters, see Table 1
k_A = mass-transfer coefficient, s^{-1}
K_{eq1} = equilibrium constant, bar^{-2}
K_{eq2} = equilibrium constant
K_{eq3} = equilibrium constant
L_R = reactor length, m
r = reaction rate, mol kg_{cat}^{-1} s^{-1}
R = gas constant, J mol^{-1} K^{-1}
S = selectivity to MeOH or DME
T = temperature, K
T_w = wall temperature, K
$u_{G,0}$ = gas superficial velocity, m s^{-1}
x_{cat} = catalyst inventory, kg_{cat} m^{-3}
X_{CO} = CO conversion
z = axial coordinate
$\Delta_R H$ = reaction enthalpy, J mol^{-1}
η_{eff} = catalyst effectiveness factor
ν = stoichiometric factor
ρ_G = gas density, kg m^{-3}

Literature Cited

1. Cote AS, Delgass WN, Ramkrishna D. Spatially patterned catalytic reactors. Feasibility issues. *Chem Eng Sci*. 2001;56:1011–1019.
2. Cote AS, Delgass WN, Ramkrishna D. Investigation of spatially patterned catalytic reactors. *Chem Eng Sci*. 1999;54:2627–2635.
3. Peng XD, Wang AW, Toseland BA, Tijm PJA. Single-step syngas-to-dimethyl ether processes for optimal productivity, minimal emissions, and natural gas-derived syngas. *Ind Eng Chem Res*. 1999;38:4381–4388.

4. Gormley RJ, Rao VUS, Anderson RR, Schehl RR, Chi RDH. Secondary reactions on metal-zeolite catalysts used in synthesis gas conversion. *J Catal*. 1988;113:193–205.
5. Iliuta I, Larachi F, Fongarland P. Dimethyl ether synthesis with in situ H_2O removal in fixed-bed membrane reactor: model and simulations. *Ind Eng Chem Res*. 2010;49:6870–6877.
6. Vanden Bussche KM, Froment GF. A steady-state kinetic model for methanol synthesis and the water gas shift reaction on a commercial $Cu/ZnO/Al_2O_3$ catalyst. *J Catal*. 1996;161:1–10.
7. Chinchen GC, Denny PJ, Parker DG, Spencer MS, Whan DA. Mechanism of methanol synthesis from $CO_2/CO/H_2$ mixtures over copper/zinc oxide/alumina catalysts: use of 14C-labelled reactants. *Appl Catal*. 1987;30:333–338.
8. Subiranas AM, Schaub G. Combining Fischer-Tropsch (FT) and hydrocarbon reactions under FT reaction conditions: model compound and combined-catalyst studies. *Int J Chem Reactor Eng*. 2009;7:A31.
9. Subiranas A, Schaub G. Combining Fischer-Tropsch (FT) and hydrocarbon reactions under FT reaction conditions—catalyst and reactor studies with Co or Fe and Pt/ZSM-5. *Int J Chem Reactor Eng*. 2007;5:A78.
10. Cote AS, Delgass WN, Ramkrishna D. *Enhancement of selective conversion in spatially patterned reactors*. In: Froment GF, Waugh KC, editors. *Studies in Surface Science and Catalysis*, Vol 122. Amsterdam: Elsevier, 1999:199–206.
11. Bercic G, Levec J. Intrinsic and global reaction rate of methanol dehydration over γ-alumina pellets. *Ind Eng Chem Res*. 1992;31:1035–1040.
12. Bercic G, Levec J. Catalytic dehydration of methanol to dimethyl ether. Kinetic investigation and reactor simulation. *Ind Eng Chem Res*. 1993;32:2478–2484.
13. Diep BT, Wainwright MS. Thermodynamic equilibrium constants for the methanol–dimethyl ether–water system. *J Chem Eng Data*. 1987;32:330–333.
14. VDI. *VDI-Wärmeatlas*, 10th ed. Düsseldorf, Germany: Springer, 2006; doi:10.1007/978-3-540-32218-4.
15. Guettel R, Turek T. Assessment of micro-structured fixed-bed reactors for highly exothermic gas-phase reactions. *Chem Eng Sci*. 2010;65:1644–1654.
16. Knochen J, Güttel R, Knobloch C, Turek T. Fischer-Tropsch synthesis in milli-structured fixed-bed reactors: experimental study and scale-up considerations. *Chem Eng Process: Process Intensification*. 2010;49:958–964.
17. Onken U, Fischer K, Rarey J. *Estimation of physical properties*. In: Pelc H, editor. *Ullmann's Encyclopedia of Industrial Chemistry*, 7th ed. Wiley, 2005; electronic resource.
18. Hayer F, Bakhtiary HD, Myrstad R, Holmen A, Pfeifer P, Venvik HJ. Synthesis of dimethyl ether from syngas in a microchannel reactor—simulation and experimental study. *Chem Eng J*. 2011;167:610–615.
19. Hu J, Wang Y, Cao C, Elliott DC, Stevens DJ, White JF. Conversion of biomass syngas to DME using a microchannel reactor. *Ind Eng Chem Res*. 2005;44:1722–1727.

Appendix

(1) Equilibrium constants

$$\log_{10}(K_{eq1}) = \frac{3066}{T} - 10.592$$

$$\log_{10}\left(\frac{1}{K_{eq2}}\right) = -\frac{2073}{T} + 2.029$$

$$\ln(K_{eq3}) = \frac{2835.2}{T} + 1.675\ln(T) - 2.39 \times 10^{-4}T - 0.21 \times 10^{-6}T^2 - 13.36$$

(2) Kinetic parameters

$$k_i(T) = A_i \exp\left(\frac{B_i}{R \times T}\right)$$

Manuscript received Nov. 1, 2011, and revision received Dec. 14, 2011.